

Photoluminescence and Structural Characteristics of Eu-doped ZnO–Li₃NbO₄

Meng-Hsi Huang, Te-Hua Fang,* Ming-Hong Lin, Chia-Wei Chang, and Yu-Cheng Fan

Department of Mechanical Engineering, National Kaohsiung University of Science and Technology,
No. 415, Jiangong Rd., Sanmin Dist., Kaohsiung City 80778, Taiwan

(Received January 19, 2019; accepted December 23, 2019)

Keywords: luminescence properties, sol–gel method, emission intensity

In this study, Eu³⁺-doped ZnO–Li₃NbO₄ phosphors were prepared by the sol–gel method. The physical and luminescence properties of the Eu³⁺-doped ZnO–Li₃NbO₄ structure were characterized. The results show the crystallinity of the biphasic ZnO–Li₃NbO₄ structure sintered at temperatures above 400 °C. The main excitation and emission bands of the Eu³⁺-doped ZnO–Li₃NbO₄ phosphors were 466 nm (⁷F₀→⁵D₂) and 615 nm (⁵D₀→⁷F₂), respectively. When the amount of Eu³⁺ was 5%, the highest emission intensity was obtained at 595 nm (⁵D₀→⁷F₁) and 615 nm (⁵D₀→⁷F₂).

1. Introduction

Zinc oxide–lithium niobate (ZnO–Li₃NbO₄) has become a popular material for application in nonlinear optical and optoelectronic devices.^(1,2) The use of a biphasic ceramic material plays an important role in optical or biomedical applications. For example, Fariña *et al.*⁽³⁾ studied biphasic calcium phosphate ceramics for biomedical and implanted applications. Bernardeschi *et al.*⁽⁴⁾ studied granules of biphasic ceramics for the rehabilitation of canal walls.

Among rare-earth-doped materials, Eu³⁺ attracts considerable scientific attention. The intra-4f-shell transitions of Eu³⁺ show that the excited levels shift the lower energy levels of ⁵D₀→⁷F_{*j*} (*j* = 1, 2, 3, 4).^(5,6) The optical properties of Eu³⁺:ZnO nanophosphors are important in material applications such as the fabrication of electroluminescence devices and biolabels.⁽⁷⁾ Ningthoujam *et al.* studied ZnO nanoparticles with and without Li⁺ and Eu³⁺ ions at low temperatures and their luminescence properties.⁽⁷⁾ Red luminescence was observed in the wavelength range of 610–620 nm.^(8,9) ZnO–Li₃NbO₄ crystals exhibit a second phase structure and could be used as a capacity rare-earth-doped host material. However, there are only a few reports on the structure and luminescence of ZnO–Li₃NbO₄ prepared by the sol–gel method.

In the present study, we synthesized Eu³⁺-doped ZnO–Li₃NbO₄ by the sol–gel method and examined its structural, optical absorption, and photoluminescence properties.

*Corresponding author: e-mail: fang@nkust.edu.tw
<https://doi.org/10.18494/SAM.2020.2595>

2. Experiments

ZnO–Li₃NbO₄:Eu powders were prepared by the sol–gel method. 99% zinc nitrate Zn(NO₃)₂, 97.7% lithium nitrate (LiNO₃), niobium ethoxide Nb(OC₂H₅)₅, and 99.8% citric acid (CA) were used as starting materials. First, stoichiometric amounts of Zn(NO₃)₂, LiNO₃, Nb(OC₂H₅)₅, europium nitrate pentahydrate (Eu(NO₃)₃·5H₂O), and CA were dissolved in distilled (D.I.) water.⁽¹⁰⁾ The precursor was dried in an oven at 150 °C for 2 h. Then, the samples were placed in an Al₂O₃ crucible and then sintered in a furnace at 400–900 °C.

The crystallinity of the samples was measured by X-ray diffraction (XRD, Rigaku D-max/IIB). The microstructure and selected-area electron diffraction (SAED) were characterized by ultrahigh-resolution analytical electron microscopy (HR-AEM, JEOL JEM-2100F CS-STEM). Absorption spectra were obtained using a UV–Vis spectrometer (Jasco V-670 spectrophotometer). The Commission internationale de l'éclairage (CIE) spectrum obtained was analyzed using a photoluminescence (PL, Hitachi F-7000) spectrometer at room temperature.

3. Results and Discussion

Figure 1(a) shows the XRD patterns of ZnO–Li₃NbO₄ synthesized at different sintering temperatures. The crystalline ZnO–Li₃NbO₄ structure was formed gradually over 400 °C (ZnO, JCPDS Card No. 89-0510, unit cell parameters: *a*, *b* = 3.249 Å and *c* = 5.206 Å, and Li₃NbO₄, JCPDS Card No. 75-0907, unit cell parameters: *a*, *b*, *c* = 8.429 Å). The main diffraction peak of 36.26° (101) appeared at different synthesis temperatures. The diffraction peak intensity of ZnO–Li₃NbO₄ with a biphasic polycrystalline structure increased with annealing temperature.

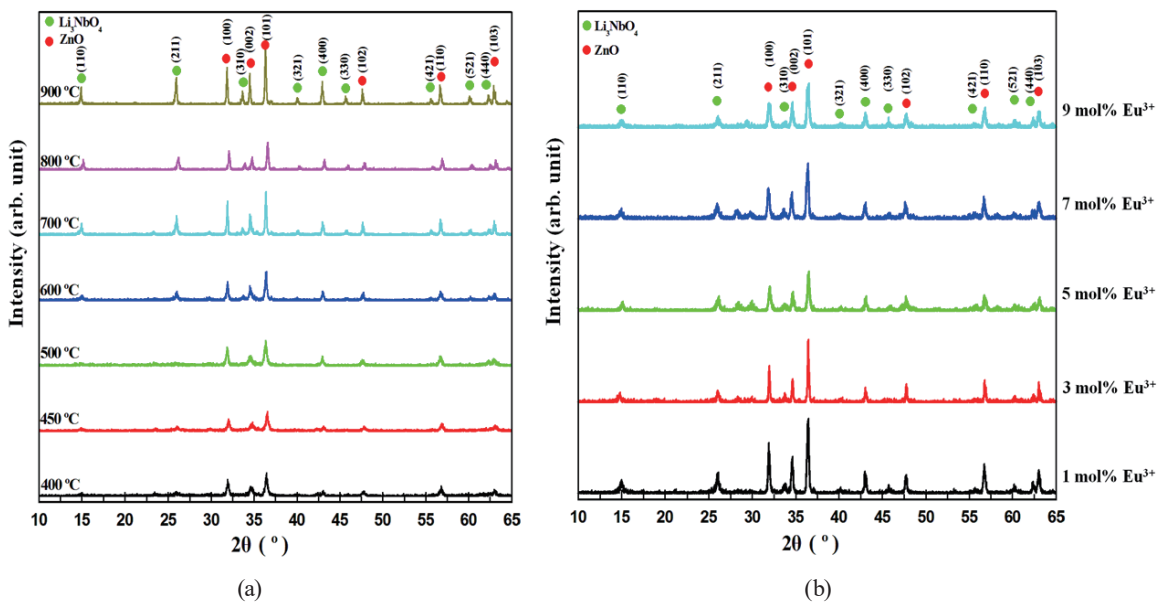


Fig. 1. (Color online) XRD patterns of ZnO–Li₃NbO₄ synthesized at different (a) sintering temperatures and (b) Eu³⁺ concentrations.

Figure 1(b) shows the XRD patterns of Eu^{3+} -doped $\text{ZnO-Li}_3\text{NbO}_4$, whose polycrystalline structure did not change. With increasing Eu^{3+} dopant concentration, the amount of $\text{ZnO-Li}_3\text{NbO}_4$ remained the same, which implies that Eu^{3+} can be integrated with a $\text{ZnO-Li}_3\text{NbO}_4$ crystal. As the concentration of Eu^{3+} increases above 7%, the crystallinity of the Eu^{3+} -doped $\text{ZnO-Li}_3\text{NbO}_4$ is expected to become lower. This phenomenon is mainly caused by structural distortion induced by internal stress.⁽¹¹⁾

Figures 2(a)–2(f) show the SEM images of $\text{ZnO-Li}_3\text{NbO}_4$ phosphors synthesized by the sol-gel method at different annealing temperatures. The $\text{ZnO-Li}_3\text{NbO}_4$ phosphors synthesized at temperatures of 400–700 °C were mostly irregular and agglomerated, and their surfaces were rough. On the other hand, the $\text{ZnO-Li}_3\text{NbO}_4$ phosphors synthesized at temperatures of

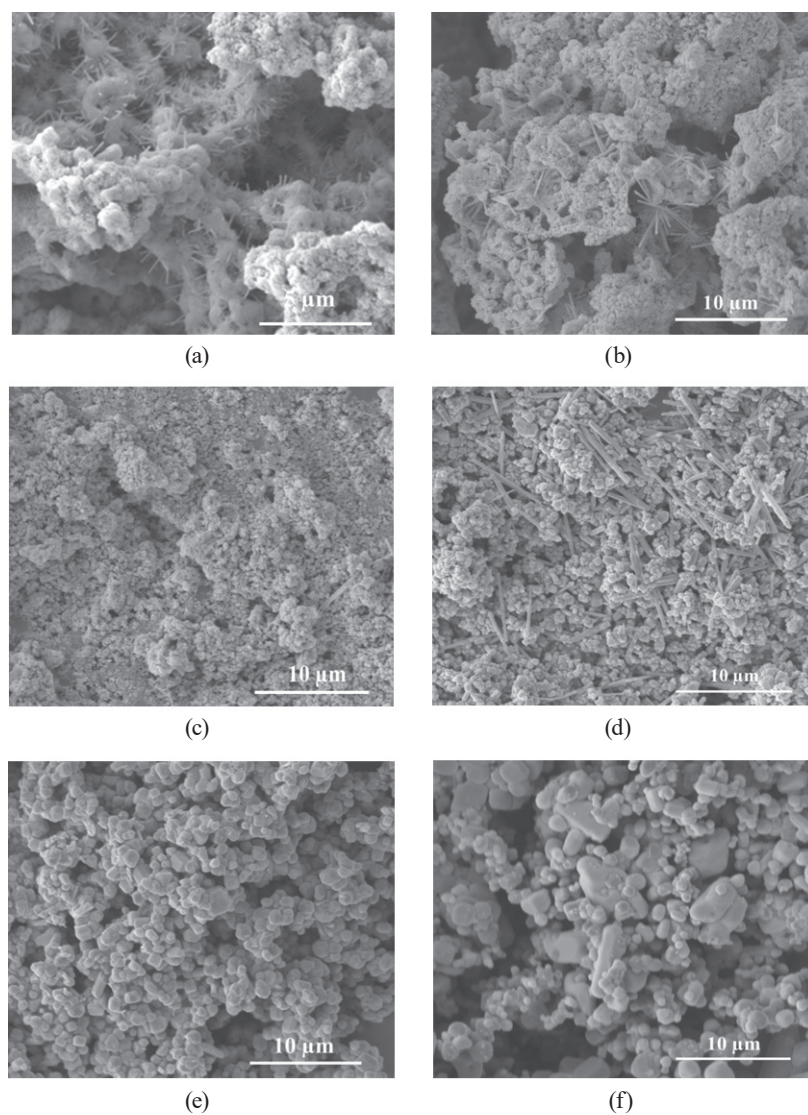


Fig. 2. SEM images of $\text{ZnO-Li}_3\text{NbO}_4$ phosphors synthesized at different annealing temperatures: (a) 400, (b) 500, (c) 600, (d) 700, (e) 800, and (f) 900 °C.

800–900 °C showed a similar particle size of about 500 nm and appeared spherical. As the temperature increased, the particle size increased. This was because the high temperature promoted the migration of atoms and the growth of pure grains, affecting the shape of the synthesized ZnO particles forming the films with increasing shape factor.⁽¹²⁾ Polygonal Li_3NbO_4 particles were formed by assembling grains with one cubic crystalline phase in the ceramic matrix.⁽¹³⁾

Figures 3(a)–3(d) show the TEM images of ZnO– Li_3NbO_4 phosphors synthesized at different temperatures. When the annealing temperature increased, the stacking and aggregation of ZnO– Li_3NbO_4 particles occurred. Figure 4(a) shows the high-resolution TEM (HR-TEM) image of ZnO– Li_3NbO_4 at an annealing temperature of 900 °C. From the HR-TEM images, the particle size was calculated to be approximately 10–50 nm. Figures 4(b) and 4(c) show the

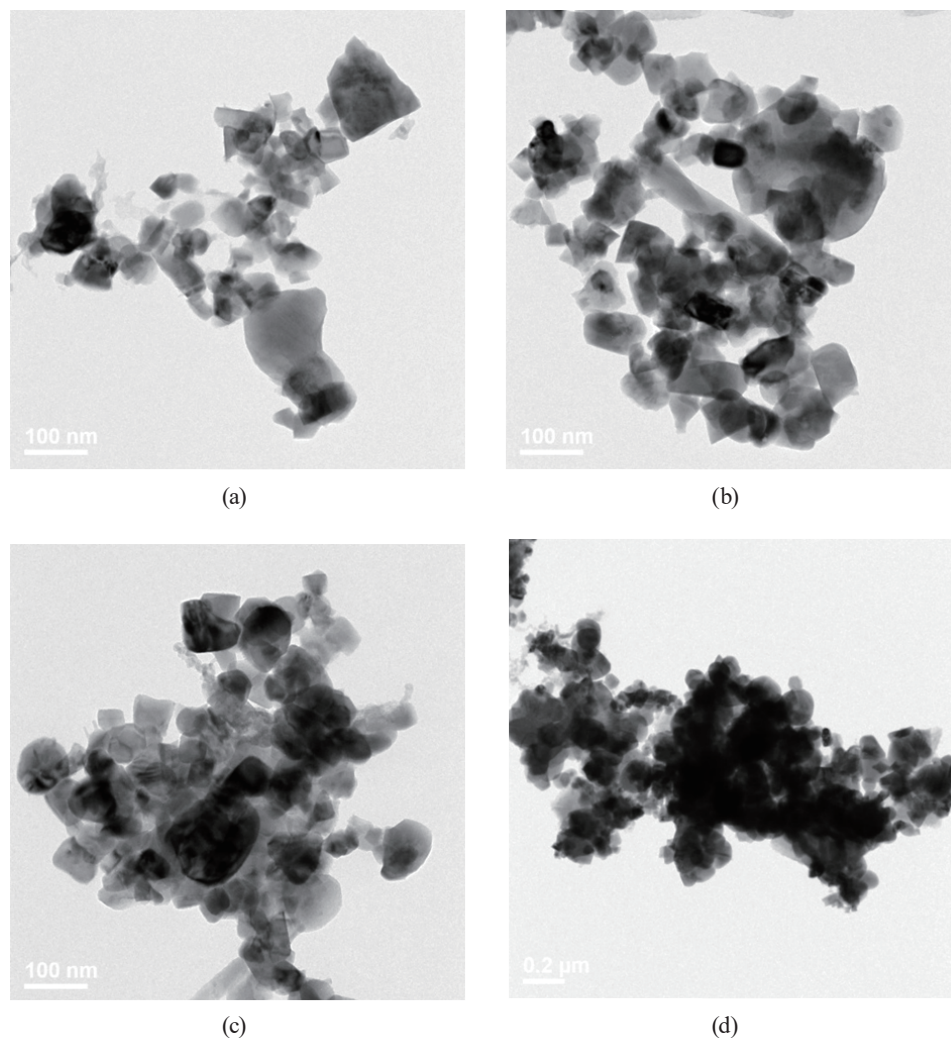


Fig. 3. TEM images of ZnO– Li_3NbO_4 phosphors synthesized at different temperatures: (a) 600, (b) 700, (c) 800, and (d) 900 °C.

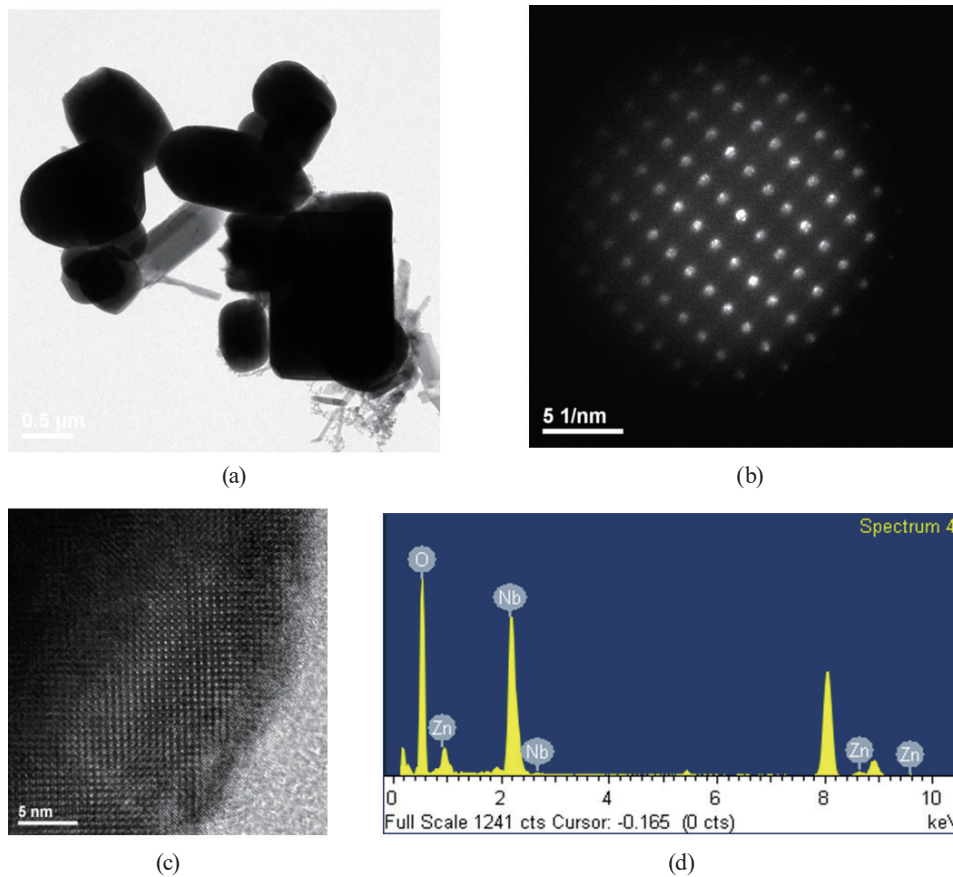


Fig. 4. (Color online) (a) HR-TEM image of pure ZnO–Li₃NbO₄ precursor powders, (b) SAED pattern of ZnO–Li₃NbO₄ annealed at 900 °C for 2 h, (c) electron diffraction pattern, and (d) EDS image.

HR-TEM and SAED patterns of ZnO–Li₃NbO₄, respectively. From the images of the lattice arrangement of ZnO–Li₃NbO₄, it can be seen that the ordering of the lattices is accurate, showing a single complete crystal structure. The lattice size was calculated to be about 0.63 nm. Figure 4(d) shows an energy-dispersive X-ray spectroscopy (EDS) image. EDS results showed the composition of ZnO–Li₃NbO₄.

Figure 5 shows the absorption spectra of ZnO–Li₃NbO₄ doped with 5 mol% Eu³⁺ and annealed at 900 °C for 2 h. The high absorption spectral peak of ZnO–Li₃NbO₄:Eu³⁺ was located between 300 and 400 nm. The absorption spectral peaks at 466 and 538 nm corresponded to ⁷F₀→⁵D₂ and ⁷F₀→⁵D₁, respectively. This behavior was attributed to the transition from the ⁷F₀ ground state to the charge transfer state (CTS).⁽¹⁰⁾ The absorption coefficient can be obtained on the basis of the relationship between $(ah\nu)^2$ and the photon energy⁽¹⁰⁾ as

$$a = \frac{C(h\nu - E_g)^{1/2}}{h\nu}, \quad (1)$$

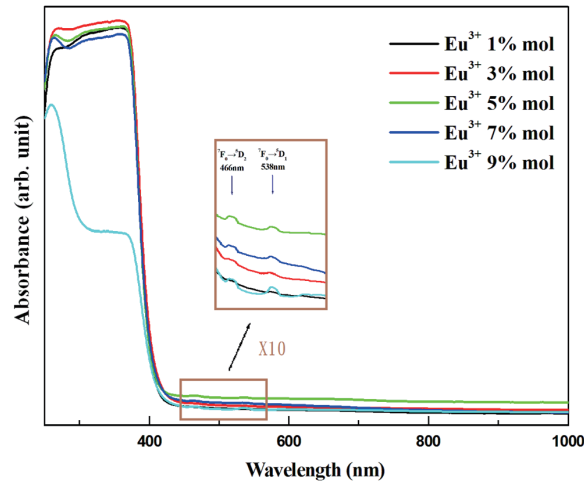


Fig. 5. (Color online) Absorption spectra of ZnO–Li₃NbO₄:xEu³⁺ ($x = 1, 3, 5, 7,$ and 9%).

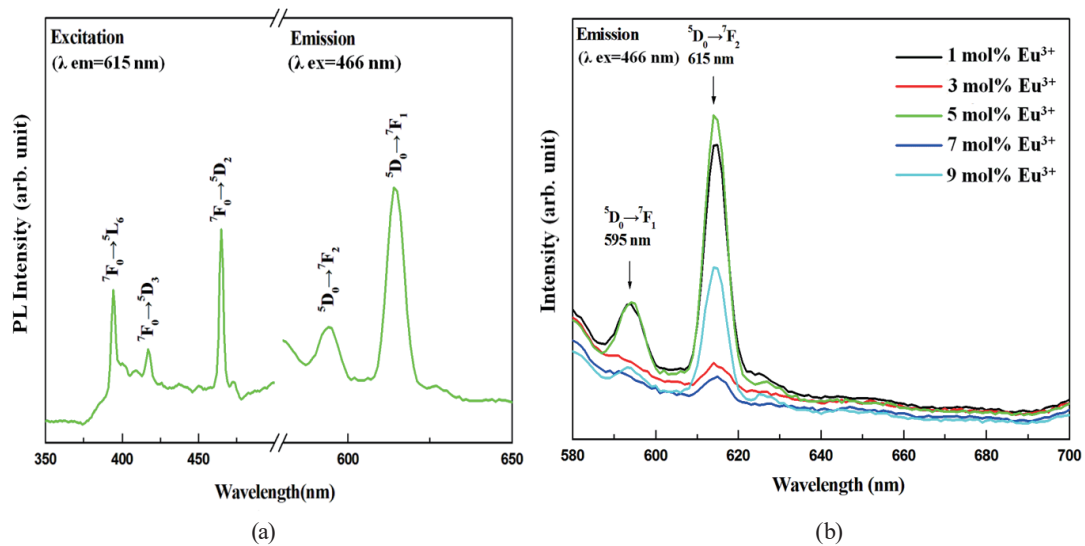


Fig. 6. (Color online) (a) Eu-doped ZnO–Li₃NbO₄ concentration-dependent PL intensity ratio of ${}^5D_0\text{--}{}^7F_1(R)/{}^5D_0\text{--}{}^7F_2(O)$. (b) Emission spectra of ZnO–Li₃NbO₄:xEu³⁺ ($x = 1, 3, 5, 7,$ and 9%).

where a is the absorption coefficient, C is a constant, $h\nu$ is the photon energy, and E_g is the energy band gap. The E_g of Eu³⁺-doped ZnO–Li₃NbO₄ was 3.13–3.24 eV. This result was similar to previously reported results.^(11,14)

Figure 6(a) shows the PL intensity–wavelength image of Eu³⁺ ions, which shows an excitation band at $\lambda_{ex} = 466$ nm (${}^7F_0\text{--}{}^5D_2$). The excitation and emission intensities of the 4f inner layer of the orbital transition of Eu³⁺-doped ZnO–Li₃NbO₄ predominantly showed the characteristic absorption peaks.⁽¹¹⁾ In the image, the first emission peak and the highest emission peak, which is classified as orange light, appear at $\lambda_{em} = 595$ nm (${}^5D_0\text{--}{}^7F_1$) and $\lambda_{em} = 615$ nm (${}^5D_0\text{--}{}^7F_2$), respectively.

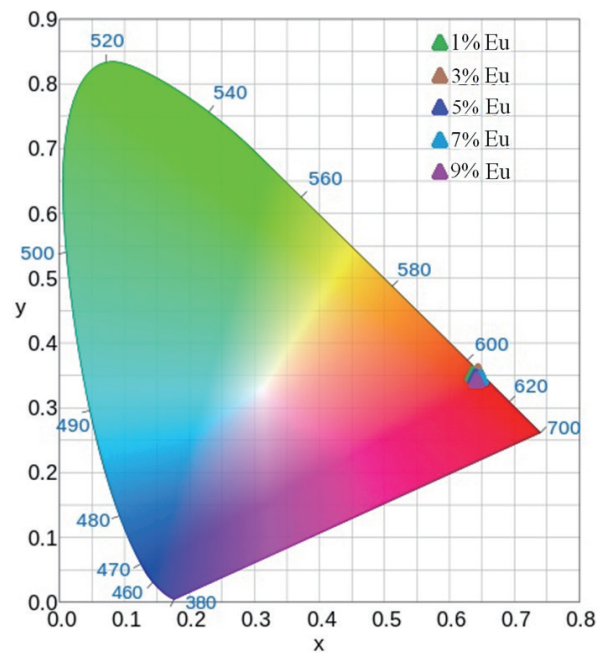


Fig. 7. (Color online) CIE color coordinate diagram of $\text{ZnO-Li}_3\text{NbO}_4:\text{xEu}^{3+}$ ($x = 1, 3, 5, 7,$ and 9%).

Figure 6(b) shows that the luminous intensity was observed to be the highest at $5\% \text{Eu}^{3+}$ and began to decrease at $7\% \text{Eu}^{3+}$. This was caused by the transfer of energy, during which the activator ion concentration saturated and reached its maximum simultaneously.⁽¹¹⁾ This revealed that the concentration of crystal defects attributed to the luminous intensity decreased during the transfer of energy. The concentration-dependent intensity ratios of ${}^5\text{D}_0 \rightarrow {}^7\text{F}_2/{}^5\text{D}_0 \rightarrow {}^7\text{F}_1$ (R/O) for 1, 3, 5, 7, and $9\% \text{Eu}^{3+}$ -doped $\text{ZnO-Li}_3\text{NbO}_4$ were 2.04, 0.92, 2.21, 0.94, and 2.12, respectively. When the concentration of the Eu^{3+} dopant was increased to 5% to form Eu^{3+} -doped $\text{ZnO-Li}_3\text{NbO}_4$, the intensity ratio (R/O) became maximum.

Figure 7 shows CIE color coordinates of $\text{ZnO-Li}_3\text{NbO}_4$ with 1 to 9 mol% Eu^{3+} doping concentrations. The CIE chromaticity coordinates show the shifted area at about $x = 0.65$ and $y = 0.35$, which was located at an orange-red light area. Such coordinates were not clearly affected by the different Eu^{3+} doping concentrations.

4. Conclusions

In this study, Eu^{3+} -doped $\text{ZnO-Li}_3\text{NbO}_4$ was successfully synthesized. XRD analysis showed that the $\text{ZnO-Li}_3\text{NbO}_4$ structure gradually formed at 400°C and the highest crystallinity was obtained at 900°C . When $5\% \text{Eu}^{3+}$ was doped into the $\text{ZnO-Li}_3\text{NbO}_4$ structure, the highest emission intensity of ${}^5\text{D}_0 \rightarrow {}^7\text{F}_1$ (466 nm) was obtained. When the CIE color coordinates of $\text{Eu}^{3+}:\text{ZnO-Li}_3\text{NbO}_4$ (about $x = 0.65$ and $y = 0.35$) were obtained, an orange-red sample was similarly observed at $5\% \text{Eu}^{3+}$. These results will be useful in the field of biological and optical detection.

Acknowledgments

This study was financially supported by the Ministry of Science and Technology (MOST), Taiwan, under Grant MOST 106-2221-E-151-026-MY3 and MOST 108CP01.

References

- 1 M. Ferrol and S. Lecocq: *Eur. J. Solid State Inorg. Chem.* **35** (1998) 10. [https://doi.org/10.1016/S0992-4361\(99\)80011-3](https://doi.org/10.1016/S0992-4361(99)80011-3)
- 2 V. A. Morozov, A. V. Arakcheeva, V. V. Konovalova, P. Pattison, G. Chapuis, O. I. Lebedev, V. V. Fomichev, and G. V. Tendeloo: *J. Solid State Chem.* **183** (2010) 2. <https://doi.org/10.1016/j.jssc.2009.12.008>
- 3 N. M. Fariña, F. M. Guzón, M. L. Peña, and A. G. Cantalapiedra: *J. Mater. Sci.-Mater. Med.* **19** (2008) 4. <https://doi.org/10.1007/s10856-008-3400-y>
- 4 D. Bernardeschi, Y. Nguyen, I. Mosnier, M. Smail, E. Ferrary, and O. Sterkers: *Eur. Arch. Otorhinolaryngol.* **271** (2014) 1. <https://doi.org/10.1007/s00405-013-2393-4>
- 5 K. B. Kim, K. W. Koo, T. Y. Cho, and H. G. Chun: *Mater. Chem. Phys.* **80** (2003) 3. [https://doi.org/10.1016/S0254-0584\(03\)00110-X](https://doi.org/10.1016/S0254-0584(03)00110-X)
- 6 Y. Wang, T. Endo, E. Xie, D. He, and B. Liu: *Microelectron. J.* **35** (2004) 4. [https://doi.org/10.1016/S0026-2692\(03\)00245-3](https://doi.org/10.1016/S0026-2692(03)00245-3)
- 7 R. S. Ningthoujam, N. S. Gajbhiye, A. Ahmed, S. S. Umre, and S. J. Sharma: *J. Nanosci. Nanotechnol.* **8** (2008) 6. <https://doi.org/10.1166/jnn.2008.152>
- 8 J. Wang, H. Hong, X. Kong, H. Peng, B. Sun, B. Chen, J. Zhang, W. Xu, and H. Xia: *J. Appl. Phys.* **93** (2003) 3. <https://doi.org/10.1063/1.1536726>
- 9 Z. Wang, D. Yuan, D. Xu, M. Lv, X. Cheng, L. Pan, and X. Shi: *J. Cryst. Growth* **255** (2003) 3. [https://doi.org/10.1016/S0022-0248\(03\)01269-7](https://doi.org/10.1016/S0022-0248(03)01269-7)
- 10 Z. W. Chiu, Y. J. Hsiao, T. H. Fang, and L. W. Ji: *J. Sol-Gel Sci. Technol.* **69** (2014) 2. <https://doi.org/10.1007/s10971-013-3215-2>
- 11 M. H. Huang, T. H. Fang, M. H. Lin, and C. W. Chang: *Mater. Res. Express* **5** (2018) 4. <https://doi.org/10.1016/j.mrex.2018.04.000>
- 12 L. Znaidi, T. Chauveau, A. Tallaire, F. Liu, M. Rahmani, V. Bockelee, D. Vrel, and P. Doppelt: *Thin Solid Films* **617** (2016) 156. <https://doi.org/10.1016/j.tsf.2015.12.031>
- 13 Y. J. Hsiao, T. H. Fang, S. J. Lin, J. M. Shieh, and L. W. Ji: *J. Lumin.* **130** (2010) 10. <https://doi.org/10.1016/j.jlumin.2010.04.023>
- 14 A. Boonchun and W. R. L. Lambrecht: *Phys. Rev. B* **81** (2010) 079904. <https://doi.org/10.1103/PhysRevB.81.235214>

About the Authors



Meng-Hsi Huang received his B.S. degree from National Pingtung University of Science and Technology, Taiwan, in 2007 and his M.S. degree from National Kaohsiung University of Applied Sciences, Taiwan, in 2014. Since 2016, he has been a Ph.D. student at National Kaohsiung University of Science and Technology, Taiwan. His research interests are in nanotechnology and fluorescent materials. (1105403105@nkust.edu.tw)



Te-Hua Fang received his B.S. degree from National Taiwan Institute of Technology, Taiwan, in 1992 and his M.S. and Ph.D. degrees from National Cheng Kung University, Taiwan, in 1994 and 2000, respectively. From 2001 to 2007, he was an assistant professor at Southern Taiwan University of Technology and National Formosa University, Taiwan. Since 2007, he has been a full professor at National Formosa University and National Kaohsiung University of Science and Technology. He is an IET Fellow. His research interests are in molecular dynamics, nanotechnology, materials, mechanics, and scanning probe microscopy. (fang.tehua@msa.hinet.net)



Ming-Hong Lin received his B.S. degree from National Taiwan Institute of Technology, Taiwan, in 1983, his M.S. degree from National Cheng Kung University, Taiwan, in 1985, and his Ph.D. degree from National Sun Yat-Sen University, Taiwan, in 1998. From 1996 to 2004, he was an assistant professor at National Kaohsiung University of Science and Technology. Since 2004, he has been a full professor at National Kaohsiung University of Science and Technology. His research interests are in mechanical materials, nanotechnology, ceramic materials, heat treatment, and surface modification. (mhlin@nkust.edu.tw)



Chia-Wei Chang received his B.S. and M.S. degrees from National Kaohsiung University of Applied Sciences, Taiwan, in 2013 and 2015, respectively. His research interest is in fluorescent materials. (allegra5202005@yahoo.com.tw)



Yu-Cheng Fan received his B.S. degree from National Kaohsiung University of Applied Sciences, Taiwan, in 2007, his M.S. degree from National Formosa University, Taiwan, in 2009, and his Ph.D. degree from National Kaohsiung University of Applied Sciences, Taiwan, in 2017. Since 2018, he has been an assistant researcher at National Kaohsiung University of Science and Technology, Taiwan. (yucheng.fan@nkust.edu.tw)